22.7 (t, J = 14, *trans*-P(CH_3)$_3$); IR (Nujol) 1418 (sh), 1343 (sh), 1299 (w), 1280 (m), 1158 (w), 1086 (w), 950 (s), 857 (m), 772 (w), 727 (m), 669 (m).

W(N^{t}Bu)(CN^{t}Bu)(PMe$_3$)$_2$Cl$_2$ (24a). In a 25-mL reaction bomb was placed 0.25 g (4.5×10^{-4} mol) of W(PMe$_3$)$_4$Cl$_2$ (**2a**). The contents of the vessel were degassed on the vacuum line, and 9 mL of dry benzene was added followed by the addition of 259 μL (1.3×10^{-3} mol) of di-*tert*-butylcarbodiimide. The reaction mixture was then stirred at 80 °C for 34 h, during which time the solution became a reddish-orange color. The volatiles were removed under vacuum giving an red-orange solid, a few milligrams of which was analyzed by ^{1}H NMR to determine the extent of reaction. The solids were taken up in 4 mL of fresh benzene, treated with 5.4 μL of additional di-*tert*-butylcarbodiimide (a 3-fold excess to react with the 5% of **2a** which remained unreacted by NMR), and heated further for 2 h. The reaction mixture was again stripped of volatiles, and the red-orange solids were scraped from the bomb. Recrystallization from toluene–diethyl ether gave ruby red crystals of **24a**: yield, 202 mg (80%); ^{1}H NMR 1.57 (18 H, t, J = 4, *trans*-P(CH_3)$_3$), 1.28 (9 H, C(CH_3)$_3$), 1.07 (9 H, C(CH_3)$_3$); ^{31}P{^{1}H} NMR −20.4 (s, *trans*-P(CH$_3$)$_3$, J_{PW} = 299); ^{13}C{^{1}H} NMR 67.6 (s, C(CH$_3$)$_3$), 61.6 (s, C(CH$_3$)$_3$), 31.7 (s, C(CH_3)$_3$), 31.4 (s, C(CH_3)$_3$), 17.0 (t, J = 14, *trans*-P(CH_3)$_3$) (the isonitrile carbon was not observed); IR (Nujol) 2012 (sh), 1916 (s), 1457 (s), 1414 (sh), 1363 (sh), 1302 (w), 1286 (w), 1280 (w), 1262 (s), 1236 (w), 1199 (s), 1039 (w), 957 (s), 855 (w), 806 (w), 739 (s), 675 (w). Anal. Calcd for $WCl_2P_2N_2C_{15}H_{36}$: C, 32.11; H, 6.47; N, 4.99. Found: C, 32.19; H, 6.31; N, 4.95.

Kinetics of Phosphine Exchange. Two solutions of Mo(PMe$_3$)$_4$Cl$_2$ (**1a**) in C_6D_6 (27 and 30 mg/mL) were prepared in NMR tubes which were attached to Teflon needle valves. The solutions were frozen (−196 °C) and degassed on the vacuum line and then treated with 12 and 40 equiv of PMe$_3$-d_9 (0.7 and 2.5 M, respectively). Upon thawing of the tubes to ambient temperature (24 ± 2 °C), the equilibration of the free deuterio and bound protio phosphine was monitored by ^{1}H NMR and found to follow the integrated rate expression $kt = 4\{[P]_e/[P]_i\} \ln \{[P]_e/([P]_e - [P]_t)\}$, where $[P]_e$ is the $[PMe_3]_{free}$ at equilibrium, $[P]_i$ is the initial amount of [PMe$_3$] bound to M(PMe$_3$)$_4$Cl$_2$, and $[P]_t$ is the $[PMe_3]_{free}$ at time t. In this expression, k is the rate constant for loss of a single phosphine from Mo(PMe$_3$)$_4$Cl$_2$; isotope effects have been neglected. The derived first-order rate constants were 6.6×10^{-4} and 6.5×10^{-4} s^{-1}, respectively, for the two runs at different concentrations of PMe$_3$-d_9.

Hammett Study of Para-Substituted Phenyl Isocyanates with 2a. A stock solution of W(PMe$_3$)$_4$Cl$_2$ (**2a**) in C_6D_6 (60.0 mg/mL) was prepared and then dispensed in 250-μL aliquots into each of the four NMR tubes followed by a 3-fold molar excess of the following isocyanates: *p*-tolyl isocyanate (10.1 μL), phenyl isocyanate (8.7 μL), 4-(trifluoromethyl)-phenyl isocyanate (11.5 μL), and 4-methoxyphenyl isocyanate (10.4 μL). An additional 250-μL aliquot of C_6D_6 was added to each tube, the tubes were degassed and sealed, and the ambient temperature reactions were monitored by ^{1}H NMR. After approximately 3 weeks, most of the **2a** in the tubes had reacted to form mixtures of tungsten oxo and imido products, identified by the similarity of their spectra to related compounds and distinguished by their respective J_{WP} values. Assignments for the ^{1}H spectra were made by ^{1}H{^{31}P} decoupling experiments.

Acknowledgment. We thank Dr. Lauren Atagi, Dr. Diana Over, and Seth Brown for their advice and Dr. Tom Pratum for assistance with some of the NMR experiments. We are grateful to the National Science Foundation for financial support.

Gated Electron-Transfer Behavior in Copper(II/I) Systems. Comparison of the Kinetics for Homogeneous Cross Reactions, NMR Self-Exchange Relaxation, and Electrochemical Data for a Copper Macrocyclic Tetrathioether Complex in Aqueous Solution

Nancy E. Meagher,[1a] Kerri L. Juntunen,[1a] Cynthia A. Salhi,[1a] L. A. Ochrymowycz,[1b] and D. B. Rorabacher*,[1a]

Contribution from the Departments of Chemistry, Wayne State University, Detroit, Michigan 48202, and University of Wisconsin—Eau Claire, Eau Claire, Wisconsin 54701. *Received May 1, 1992*

Abstract: The kinetics of electron-transfer reactions involving Cu$^{II/I}$([14]aneS$_4$) reacting with a series of selected counterreagents have been measured in aqueous solution at 25 °C, μ = 0.10 M (ClO_4^-). The reagents utilized include four oxidants [Ru(NH$_3$)$_4$bpy^{3+}, Ni([14]aneN$_4$)$^{3+}$, Ru(NH$_3$)$_2$(bpy)$_2^{3+}$, and Fe(4,7-Me$_2$phen)$_3^{3+}$] and four reductants [Co(Me$_4$[14]tetraeneN$_4$)$^{2+}$, Ru(NH$_3$)$_4$bpy^{2+}, Ru(NH$_3$)$_5$isn^{2+}, and Ru(NH$_3$)$_5$py^{2+}], which were selected to provide a variety of reagent self-exchange rate constants and overall reaction potentials, thereby yielding a range of cross reaction rate constant values. Application of the Marcus equation to the cross reaction rate constants for the four *reduction* studies yielded consistent self-exchange rate constant values of log $k_{11(red)}$ = 3.78 (±0.26) for Cu$^{II/I}$([14]aneS$_4$). By contrast, the two *oxidation* kinetic studies having the largest reaction potentials [i.e., using Ru(NH$_3$)$_2$(bpy)$_2^{3+}$ and Fe(4,7-Me$_2$phen)$_3^{3+}$ as oxidants] yielded log $k_{11(ox)} \approx 0$ (±0.26), while the *oxidation* reactions with smaller reaction potentials [i.e., using Ru(NH$_3$)$_4$bpy^{3+} and Ni([14]aneN$_4$)$^{3+}$ as oxidants] yielded an apparent value of log $k_{11(ox)} \approx 2.5$ for Cu$^{II/I}$([14]aneS$_4$) when *relatively small concentrations* of the counteroxidant were used. Upon an increase in the Ni([14]aneN$_4$)$^{3+}$ concentration, however, $k_{11(ox)}$ appeared to decrease until, at relatively high concentrations of the Ni(III) reagent, limiting first-order kinetic behavior was observed. In an independent study, NMR line-broadening measurements were made on Cu^I([14]aneS$_4$) solutions containing variable amounts of Cu^{II}([14]aneS$_4$) to obtain a direct measurement of log $k_{11(ex)} \approx 3.88 \pm 0.09$ at 25 °C ($\Delta H^{\ddagger} = 20.7 \pm 4.5$ kJ mol^{-1}; $\Delta S^{\ddagger} = -101 \pm 13$ J K^{-1} mol^{-1}). This is in direct agreement with the values calculated from the reduction reactions. The patterns in the kinetic behavior of Cu$^{II/I}$([14]aneS$_4$) are shown to be consistent with a dual-pathway square scheme, as characterized by rapid-scan cyclic voltammetry. For Cu^{I}L oxidation reactions, the conformational change to form a metastable Cu^{I}L species becomes rate-limiting under specific conditions, resulting in the appearance of "gated" electron-transfer kinetics; ultimately, the oxidation reaction switches to the alternate reaction pathway.

Introduction

In previous work we have reported the results of homogeneous electron-transfer kinetic studies on both the oxidation and reduction of Cu(II)/(I) complexes involving an entire series of macrocyclic and acyclic polythioethers (L).[2] In that investigation,

(1) (a) Wayne State University. (b) University of Wisconsin—Eau Claire.

(2) Martin, M. J.; Endicott, J. F.; Ochrymowycz, L. A.; Rorabacher, D. B. *Inorg. Chem.* **1987**, *26*, 3012-3022.

0002-7863/92/1514-10411$03.00/0

Scheme I

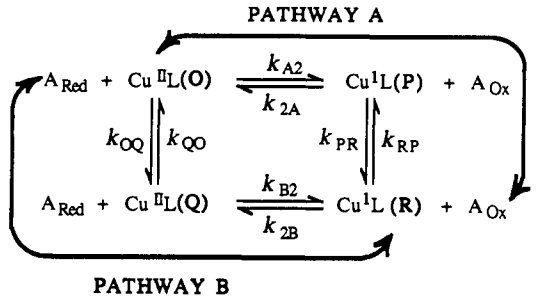

we noted that the application of the Marcus relationship[3-6] to evaluate the apparent values of the self-exchange rate constants of the Cu(II)/(I) couples yielded much *larger* values for reactions in which $Cu^{II}L$ was being *reduced* ($k_{11(red)}$) than for reactions in which $Cu^{I}L$ was being *oxidized* ($k_{11(ox)}$). We proposed that the apparent inconsistencies in the electron-transfer behavior of Cu(II)/(I) systems are the result of a dual-pathway ("square scheme") mechanism.[2,7] As a result of the differences in the thermodynamic parameters for reactions favoring $Cu^{II}L$ reduction and those favoring $Cu^{I}L$ oxidation, the preferred reaction pathway appears to change with differing counterreagents.[8]

As illustrated in Scheme I for homogeneous cross reactions, the proposed square scheme involves metastable conformers (or configurations), designated as $Cu^{II}L(Q)$ and $Cu^{I}L(P)$, which are presumed to more nearly approximate the geometry of the stable conformers (or configurations) of the opposite oxidation state. As a result, the intermediate species are more easily reduced and oxidized than the corresponding stable species, $Cu^{II}L(O)$ and $Cu^{I}L(R)$, respectively. For such a mechanism, the preferred pathway for a cross reaction with a selected counterreagent, A_{red} or A_{ox}, *carried out under conditions where all species are fully equilibrated*, should be determined solely by the relative stability of the metastable intermediate species, Q and P. Under these conditions, the normal Marcus relationship will apply and no direct evidence for a square scheme mechanism should be observed. As the reaction potential and/or the self-exchange rate constant (or concentration) of the counterreagent increases, however, the rate of the electron-transfer step will ultimately exceed the rate of conformational change. At that point, conformational change will become rate-limiting and the overall reaction will appear to be first order, independent of the counterreagent. Interestingly, for reactions which are thermodynamically favorable, this latter situation will occur only for the condition where conformational change precedes the electron-transfer step.

The significance of electron-transfer mechanisms of the type shown in Scheme I, in which electron transfer and conformational change occur as sequential, rather than concerted, processes, has gained increasing attention in recent years, particularly as it pertains to biological processes involving metalloenzymes. Hoffman and Ratner[9,10] and Brunschwig and Sutin[11,12] have recently presented general theoretical treatments for the electron-transfer behavior of systems which conform to square schemes, such as that shown in Scheme I. In so doing, they have particularly noted the possibility that the conformational changes involved in forming metastable intermediates can become rate-limiting *in one direction*, leading to a situation which they have termed "gated"[9,10] or "directional"[11,12] electron transfer. Since the conformationally-controlled "gating" places an upper limit on the rate of electron transfer (within certain limiting conditions), it has been suggested that this phenomenon may be of particular importance in controlling the back reactions of enzymatic processes[11,12] resulting in a so-called "molecular switch".[13]

Evidence for the existence of conformational change as the rate-limiting process in redox-active metalloenzymes has been mounting, particularly in intra- and intermolecular electron-transfer reactions of heme proteins and cytochrome *c* oxidase.[14-19] Limiting first-order kinetics ascribed to conformational changes have also been reported for type 1 copper sites in two blue copper proteins, azurin[20,21] and rusticyanin.[22] However, such systems do not readily lend themselves to detailed electrochemical measurements or other independent approaches for evaluating the rate constants associated with conformationally-limiting processes.

In our laboratories, both low-temperature[23] and rapid-scan[24] cyclic voltammetric measurements on the copper complex formed with the macrocyclic ligand 1,4,8,11-tetrathiacyclotetradecane ([14]aneS$_4$) have now provided direct evidence for the existence

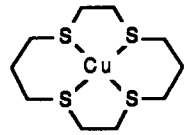

of metastable forms of both the $Cu^{II}L$ and $Cu^{I}L$ species, thereby providing support for the existence of our proposed dual-pathway ("square scheme") mechanism for electron transfer. Moreover, the use of the rapid-scan technique has now made it possible to estimate the rate constants (in 80% methanol) associated with the individual conformational changes, labeled k_{OQ}, k_{QO}, k_{PR}, and k_{RP} in Scheme I.[24] Therefore, we are now in a position to test the validity of Scheme I for homogeneous electron-transfer reactions with this specific Cu(II)/(I) system.

In the current study, we have completed a thorough kinetic investigation of cross reactions involving both the reduction and oxidation of the $Cu^{II/I}$([14]aneS$_4$) complex (eq 1) using coun-

$$Cu^{II}L + A_{red} \underset{k_{21}}{\overset{k_{12}}{\rightleftharpoons}} Cu^{I}L + A_{ox} \qquad (1)$$

terreagents (A_{red}, A_{ox}) with a variety of potentials and self-ex-

(3) Marcus, R. A. *J. Chem. Phys.* **1956**, *24*, 966-978.
(4) Marcus, R. A. *Discuss. Faraday Soc.* **1960**, *29*, 21-31.
(5) Marcus, R. A. *J. Chem. Phys.* **1965**, *43*, 679-701.
(6) Marcus, R. A.; Sutin, N. *Biochim. Biophys. Acta* **1985**, *811*, 265-322.
(7) Rorabacher, D. B.; Bernardo, M. M.; Vande Linde, A. M. Q.; Leggett, G. H.; Westerby, B. C.; Martin, M. J.; Ochrymowycz, L. A. *Pure Appl. Chem.* **1988**, *60*, 501-508.
(8) As noted in this work, changes in reagent concentration may bring about a change in the preferred reaction pathway. Since reactions studied in both directions using the same counterreagent always require differing reactant concentrations when forcing the reaction in one direction or the other, observed changes in the apparent pathway do not violate microscopic reversibility.
(9) Hoffman, B. M.; Ratner, M. A. *J. Am. Chem. Soc.* **1987**, *109*, 6237-6243. Cf., correction: *Ibid.* **1988**, *110*, 8267.
(10) Hoffman, B. M.; Rattner, M. A.; Wallin, S. A. In *Electron Transfer in Biology and the Solid State*; Johnson, M. K., King, R. B., Kurtz, D. M., Jr., Kutal, C., Norton, M. L., Scott, R. A., Eds.; American Chemical Society: Washington, DC, 1990; Vol. 226, pp 125-146.
(11) Brunschwig, B. S.; Sutin, N. *J. Am. Chem. Soc.* **1989**, *111*, 7454-7465.
(12) Sutin, N.; Brunschwig, B. S. In *Electron Transfer in Biology and the Solid State*; Johnson, M. K., King, R. B., Kurtz, D. M., Jr., Kutal, C., Norton, M. L., Scott, R. A., Eds.; American Chemical Society: Washington, DC, 1990; Vol. 226, pp 65-88.
(13) Pratt, J. M. *J. Inorg. Biochem.* **1986**, *28*, 145-153.
(14) Bechtold, R.; Kuehn, C.; Lepre, C.; Isied, S. S. *Nature* **1986**, *322*, 286-288.
(15) Feitelson, J.; McLendon, G. *Biochemistry* **1991**, *30*, 5051-5055.
(16) Isied, S. S. In *Electron Transfer in Biology and the Solid State*; Johnson, M. K., King, R. B., Kurtz, D. M., Jr., Kutal, C., Norton, M. L., Scott, R. A., Eds.; American Chemical Society: Washington, DC, 1990; Vol. 226, pp 91-100.
(17) Malmstrom, B. G.; Nilsson, T. *Ann. N. Y. Acad. Sci.* **1988**, *550*, 177-184.
(18) Nocek, J. M.; Liang, N.; Wallin, S. A.; Mauk, A. G.; Hoffman, B. M. *J. Am. Chem. Soc.* **1990**, *112*, 1623-1625.
(19) Wilson, M. T.; Alleyne, T.; Clague, M.; Conroy, K.; El-Agez, B. *Ann. N. Y. Acad. Sci.* **1988**, *550*, 167-176.
(20) Rosen, P.; Pecht, I. *Biochemistry* **1976**, *15*, 775-786.
(21) Silvestrini, M. C.; Brunori, M.; Wilson, M. T.; Darley-Usmar, V. M. *J. Inorg. Biochem.* **1981**, *14*, 327-338.
(22) Lappin, A. G.; Lewis, C. A.; Ingledew, C. A. *Inorg. Chem.* **1985**, *24*, 1446-1450.
(23) Bernardo, M. M.; Robandt, P. V.; Schroeder, R. R.; Rorabacher, D. B. *J. Am. Chem. Soc.* **1989**, *111*, 1224-1231.
(24) Robandt, P. V.; Schroeder, R. R.; Rorabacher, D. B. To be submitted for publication.

change rate constants. The primary focus of this study is aimed at determining whether the kinetic behavior of this $Cu^{II/I}L$ couple is dependent upon the properties of the counterreagents in a manner consistent with the conditions which should bring about gated electron transfer. In addition to our electrochemical measurements,[24] we have also obtained direct measurements on the self-exchange rate constant for this same copper(II)/(I) system, as represented in eq 2, using NMR line-broadening techniques.

$$*Cu^{II}L + Cu^{I}L \underset{}{\overset{k_{11(ex)}}{\rightleftharpoons}} *Cu^{I}L + Cu^{II}L \qquad (2)$$

The results of these studies provide the first definitive demonstration of gated electron transfer under conditions which can be independently confirmed from the combined evidence of electrochemical measurements,[24,25] self-exchange relaxation, and cross reaction kinetics.

Experimental Section

Reagents. The preparation of pure crystalline $Cu(ClO_4)_2$, used as the copper salt in all cross reactions, has been previously reported.[26] Reagent grade copper(II) nitrate, used for the NMR line-broadening studies, was recrystallized twice from water, filtered, and dried in a vacuum desiccator to yield $Cu(NO_3)_2 \cdot 3H_2O$. (The waters of crystallization did not significantly affect the NMR spectral data.) Copper metal shot (99.90%, Allied Chemical Corp.), used for the reduction of $Cu^{II}L$ to the corresponding $Cu^{I}L$ species, was cleaned with dilute reagent grade nitric acid, rinsed twice with distilled deionized water, rinsed with methanol, dried in an oven for 7–10 min, and stored in a desiccator for 10 min before use. The synthesis of the [14]aneS$_4$ ligand has been previously published.[27] For the ^{1}H NMR measurements, deuterium oxide (99.8% D) was obtained from Aldrich Chemical Company and chloroform-*d* (99.8% D), used for obtaining the ligand spectrum, was obtained from Stohler Isotope Chemicals. For all other studies, distilled deionized water was used.

Of the counterreagents utilized in this work, $[Fe(4,7\text{-}Me_2phen)_3](ClO_4)_3 \cdot 3H_2O$ (4,7-Me$_2$phen = 4,7-dimethyl-1,10-phenanthroline) was prepared by the method of Ford-Smith and Sutin.[28] The reagent $[Ni([14]aneN_4)(H_2O)_2]Cl_2$ ([14]aneN$_4$ or cyclam = 1,4,8,11-tetraazacyclotetradecane) was prepared by the method of Barefield et al.[29] and was subsequently oxidized to the Ni(III) salt using PbO_2. Commercially available $[Ru(NH_3)_5Cl]Cl_2$ (Strem Chemicals, Inc.) was used as the starting material for the synthesis of all ruthenium reagents. The compound $[Ru(NH_3)_5py](ClO_4)_2$ (py = pyridine) was prepared using the method outlined by Gaunder and Taube[30] with modifications developed by Cummins and Gray.[31] (**WARNING!** *$[Ru(NH_3)_5py](ClO_4)_2$ is shock sensitive when dry; any filtration of the solid should be done using filter paper, not a sintered glass filter funnel; the material should not be thoroughly dried and should be handled with caution.*) The initial product was subsequently oxidized with ceric perchlorate in acetone to $Ru^{III}(NH_3)_5py$. After oxidation, the acetone was removed with a rotary evaporator, yielding a pale yellow precipitate, which was recrystallized from warm aqueous 0.1 M $HClO_4$ and washed with cold 0.1 M $HClO_4$. The purified solid was stored in a refrigerator and protected from light. Zinc amalgam was subsequently used to reduce this material to $Ru^{II}(NH_3)_5py$ as needed.

The related compound $[Ru(NH_3)_5isn](ClO_4)_3$ (isn = isonicotinamide) was prepared by modifying the method of Gaunder and Taube[30] as follows. After preparation of $[Ru(NH_3)_5H_2O](CF_3SO_3)_3$, this latter material was mixed with a 50% molar excess of isonicotinamide in the minimum amount of methanol required for dissolution. The mixture was protected from light while being purged with argon over zinc amalgam for 3 h. The dark red-orange solution was decanted from the amalgam and quickly filtered for any undissolved solids. The filtrate was then acidified with 1 M $HClO_4$ and the complex oxidized by adding PbO_2 and stirring for approximately 5 min. Excess PbO_2 was filtered from the bright yellow solution with glass wool. The solution volume was reduced by vacuum, and a small amount of solid $NaClO_4$ was added to initiate the precipitation of $[Ru(NH_3)_5isn](ClO_4)_3$ as a yellow powder, which was then filtered and air dried. The divalent compound was prepared, as needed, by reduction with zinc amalgam.

The compounds $[Ru(NH_3)_4bpy](ClO_4)_2$ and *cis*-$[Ru(NH_3)_2(bpy)_2](ClO_4)_2$ (bpy = 2,2′-bipyridine) were prepared by the methods of Brown and Sutin[32] and Bryant et al.,[33] respectively. The corresponding tervalent compounds were prepared by oxidizing the divalent compounds over PbO_2 as described by Brown and Sutin.[32] For all of the foregoing reagents, the final products of the syntheses were checked by comparing their spectral properties against the literature values. In a number of cases, the redox properties of the synthesized compounds were also checked by cyclic voltammetry.

Preparation of Solutions. Solutions of $Cu^{II}L$ complexes for the NMR studies were prepared by transferring the desired amount of deuterated water to a 10-mL volumetric flask (sealed with a septum to exclude the condensation of water vapor from the air) which contained a weighed mixture of copper(II) nitrate and the appropriate ligand. The resulting solutions were stirred overnight, and their concentrations were checked spectrophotometrically at 25 °C using a 1-mm quartz cell.

Since the potential of $Cu^{II/I}([14]aneS_4)$ is such that the $Cu^{I}L$ complex is stable with respect to disproportionation,[25] clean copper shot was used to reduce $Cu^{II}L$ to $Cu^{I}L$ according to the reaction

$$Cu^{II}L + Cu^0 + L \rightarrow 2Cu^{I}L \qquad (3)$$

To ensure complete reduction, reaction 3 was carried out overnight in an oxygen-free environment. By preparing solutions containing initially a 1:2 ratio of $[Cu^{II}_{aq}]$:[L], the only product obtained from reaction 3 was pure $Cu^{I}L$, which could be easily removed from the excess copper shot. [NOTE: If additional Cu^{II}_{aq} is present *prior to the addition of the elemental copper*, a significant amount of Cu^{I}_{aq} is generated (on the order of 10^{-4} M); in the NMR experiments, in which $Cu^{I}L$ is mixed with $Cu^{II}L$ in the NMR tubes, excess Cu^{I}_{aq} can undergo either ligand exchange or electron transfer with the $Cu^{II}L$ to decrease $[Cu^{II}L]$ and increase $[Cu^{I}L]$, thereby affecting the subsequent line widths.] All solutions containing $Cu^{I}L$ and/or $Cu^{II}L$ were stored under dried oxygen-free argon gas and were transferred from one vessel to another using gastight syringes (Hamilton 1000 series).

For each series of NMR line-broadening measurements, six samples containing constant amounts of $Cu^{I}L$ but varying concentrations of $Cu^{II}L$ were prepared. In view of the weak complexing ability of the [14]aneS$_4$ ligand,[34,35] most of the $Cu^{II}L$ solutions prepared in this manner contained a large excess of $Cu(NO_3)_2$ to ensure complete complexation of the ligand. Each NMR tube was stoppered to minimize air oxidation during the line-broadening measurements, and all measurements were made within 24 h of solution preparation.

Instrumentation. All ^{1}H NMR spectra for line-broadening experiments and T_1 relaxation measurements were recorded on a Nicolet GN 300-MHz spectrometer equipped with a variable temperature unit and a Nicolet NMC 1280 data system. Other NMR measurements, such as homonuclear decoupling and ^{13}C spectral determinations, were recorded on a GE QE 300-MHz spectrometer. The cross reaction kinetic measurements were made using a Durrum D-110 stopped-flow spectrophotometer interfaced to an Eltech Turbo XT computer equipped with a Metrabyte 12-bit A/D board. Visible absorption measurements, used to check the concentrations of $Cu^{II}L$ solutions, were made using a Cary 17D double-beam recording spectrophotometer. All pH measurements were conducted with an Orion Model 901A digital analyzer using a micro Ag/AgCl pH combination electrode.

NMR Measurements. For all line-broadening experiments, a one-pulse sequence was used for the acquisition of the free induction decay (FID) signal. Shimming on the FID was used in order to ensure a homogeneous field. The following parameters were employed in this study: 100 pulses; 25-μs pulse length; 4.5-s delay time; 2-s acquisition time; sweep width (SW) = ±2000 Hz; block size = 16K. The NMR spectrum for each tube was recorded at four temperatures corresponding to 5, 15, 25, and 35 °C. The specific concentration of $Cu^{II}L$ in each tube was checked spectrophotometrically at 390 nm, following completion of the NMR measurements, by transferring the solutions to low-volume 1-cm cells. Since overlapping peaks were used in some instances, the peak line widths were determined using the Curve Analysis Program (CAP).[36] For T_1

(25) Bernardo, M. M.; Schroeder, R. R.; Rorabacher, D. B. *Inorg. Chem.* **1991**, *30*, 1241–1247.
(26) Diaddario, L. L.; Zimmer, L. L.; Jones, T. E.; Sokol, L. S. W. L.; Cruz, R. B.; Yee, E. L.; Ochrymowycz, L. A.; Rorabacher, D. B. *J. Am. Chem. Soc.* **1979**, *101*, 3511–3520.
(27) Ochrymowycz, L. A.; Mak, C. P.; Michna, J. D. *J. Org. Chem.* **1974**, *39*, 2079–2084.
(28) Ford-Smith, M. H.; Sutin, N. *J. Am. Chem. Soc.* **1961**, *83*, 1830–1834.
(29) Barefield, E. K.; Wagner, F.; Herlinger, A. W.; Dahl, A. R. *Inorg. Synth.* **1976**, *16*, 220–224.
(30) Gaunder, R. G.; Taube, H. *Inorg. Chem.* **1970**, *9*, 2627–2639.
(31) Cummins, D.; Gray, H. B. *J. Am. Chem. Soc.* **1977**, *99*, 5158–5167.
(32) Brown, G. M.; Sutin, N. *J. Am. Chem. Soc.* **1979**, *101*, 883–892.
(33) Bryant, G. M.; Fergusson, J. E.; Powell, H. K. J. *Aust. J. Chem.* **1971**, *24*, 257–273.
(34) Sokol, L. S. W. L.; Ochrymowycz, L. A.; Rorabacher, D. B. *Inorg. Chem.* **1981**, *20*, 3189–3195.
(35) Young, I. R.; Ochrymowycz, L. A.; Rorabacher, D. B. *Inorg. Chem.* **1986**, *25*, 2576–2582.

relaxation measurements, the inversion recovery (T1IR) method was used.[37]

Results

Data Treatment for Stopped-Flow Kinetic Measurements. For the cross reactions included in this work (reaction 1), counter-reagents (A_{red} and A_{ox}) were selected to provide a wide variety of reaction potentials ranging from negative values (i.e., thermodynamically unfavorable reactions) to large positive values (resulting in very rapid reactions). All reactions involved stoichiometric one-electron transfer. To facilitate the study of very rapid reactions, in particular, the kinetics were generally measured under conditions where neither reactant was present in large excess (i.e., pseudo-first-order conditions were generally avoided). The kinetics for all such reactions were treated using the general reversible second-order expression:

$$dX/dt = k_{12}[A][B] - k_{21}[C][D] \quad (4)$$

In relation to reaction 1, the terms [A], [B], [C], and [D] correspond to the molar concentrations of $Cu^{II}L$, A_{red}, $Cu^{I}L$, and A_{ox}, respectively, at any time t. For reactions involving the reduction of $Cu^{II}L$, the quantity X was then defined as the extent of reaction from the time defined as $t = 0$ to any later time,

$$X = [A]_0 - [A] = [B]_0 - [B] = [C] - [C]_0 = [D] - [D]_0 \quad (5)$$

where the zero subscripts designate the concentration values at the selected zero time. (For reactions involving the oxidation of $Cu^{I}L$, the value of X has the opposite sign and all equations still apply.) Due to the occurrence of some air oxidation of the reduced reagent, A_{red} (and/or $Cu^{I}L$), prior to the initiation of the reaction, and/or to the poorly characterized initial kinetic behavior when the reaction mean lifetime did not greatly exceed the instrumental mixing time (a condition which was prevalent for very fast reactions, vide infra), the values of $[C]_0$ and/or $[D]_0$ were frequently significant.

Using the subscript e to designate concentration values existing at thermodynamic equilibrium, it is apparent, by definition, that $dX_e/dt = 0$ and

$$k_{12}[A]_e[B]_e = k_{21}[C]_e[D]_e \quad (6)$$

or, upon rearrangement,

$$k_{21} = k_{12}[A]_e[B]_e/[C]_e[D]_e \quad (7)$$

Substitution of eq 7 into eq 4 yields, upon rearrangement and separation of the variables,

$$\frac{dX\,[C]_e[D]_e}{[A][B][C]_e[D]_e - [C][D][A]_e[B]_e} = k_{12}\,dt \quad (8)$$

Insertion of the relationships defined in eq 5 into this latter expression permits eq 8 to be expressed in terms of the single variable X. The resultant equation can then be integrated in the form

$$[C]_e[D]_e \int_{X_0}^{X_t} \frac{dX}{aX^2 + bX + c} = k_{12} \int_0^t dt$$

to yield the following final expression:[38]

$$\frac{[C]_e[D]_e}{(b^2 - 4ac)^{1/2}} \left[\ln \left(\frac{2aX_t + b - (b^2 - 4ac)^{1/2}}{2aX_t + b + (b^2 - 4ac)^{1/2}} \right) - \ln \left(\frac{2aX_0 + b - (b^2 - 4ac)^{1/2}}{2aX_0 + b + (b^2 - 4ac)^{1/2}} \right) \right] = k_{12}t \quad (9)$$

where X_t represents the change in molar concentration of each of the reactants and products at any time t relative to their values at the selected zero time. The other variables in eq 9 are defined as

$$a = [C]_e[D]_e - [A]_e[B]_e$$

$$b = -\{([A]_0 + [B]_0)[C]_e[D]_e + ([C]_0 + [D]_0)[A]_e[B]_e\}$$

$$c = [A]_0[B]_0[C]_e[D]_e - [A]_e[B]_e[C]_0[D]_0$$

A computer program was written to solve eq 9 for k_{12} from the experimental absorbance (Abs) data using the relationship

$$X_t = \frac{\mathrm{Abs}/l - \epsilon_A[A]_0 - \epsilon_B[B]_0 - \epsilon_C[C]_0 - \epsilon_D[D]_0}{\epsilon_C + \epsilon_D - \epsilon_A - \epsilon_B}$$

where l represents the cell path length (cm) and the ϵ terms represent the molar absorptivity values for each of the respective species at the selected wavelength used for monitoring the reaction. In utilizing eq 9, the data for times close to the instrumental dead time (approximately 3.5 ms) were automatically discarded. The data for the next 10% of the remaining total absorbance change were also generally omitted from the data analysis (as were the final 10%), and the first point thereafter was defined as $t = 0$. The values of $[A]_0$, $[B]_0$, $[C]_0$, and $[D]_0$ were calculated on the basis of the known initial concentrations prior to mixing and the experimental absorbance value at the selected zero time. Usually, it was necessary to correct for slight air oxidation of the reduced reagent which occurred prior to and/or subsequent to the filling of the drive syringes. This was accomplished by arbitrarily adjusting the initial concentration value until an optimal fit to eq 9 was obtained. Such corrections, when made, were generally small and always in the direction anticipated for air oxidation.[39]

It should be noted that eq 9 is general in nature and is valid both for reactions which proceed to completion and for reactions in which no significant amount of product has been formed at the selected zero time. Thus, this expression is more complex than is necessary for many of the reactions included in this study. Nonetheless, the use of this general expression provides many advantages, particularly with respect to the fact that no prejudicial decisions are required regarding the necessity for making corrections for initial product formation or the failure of the reaction to proceed to completion. In applying this treatment, however, it should be noted that absolute (rather than relative) values for the absorbance must be obtained. Thus, careful calibration of the instrument is essential.

For very fast reactions having mean lifetimes within an order of magnitude of the time required to fill the cell of the stopped-flow spectrophotometer, a significant concentration gradient exists along the monitored path length during the early part of the reaction. Since fractional lifetimes for second-order reactions are dependent upon the initial concentrations at the selected zero time, the concentration gradient within the cell may result in significant errors when one attempts to analyze the data. Previously we have corrected for such inhomogeneities under conditions where $[A]_0 = [B]_0$, $[C]_0 = [D]_0 = 0$, and the reverse reaction is insignificant.[40] In the current studies, however, the prevalence of (i) some air oxidation of the reduced reagent prior to the initiation of the reaction runs and/or (ii) the significant contribution of the reverse reaction in eq 4 tended to make it impractical to maintain these limiting conditions. Experimentation with various approaches to the data treatment resulted in the conclusion that, for the fastest reactions studied, the concentration gradient problems within the cell could be rendered inconsequential by selecting $t = 0$ at a point where problems caused by the gradient within the monitored path length had diminished to a low level.[41] This point could generally

(36) NMC-1280 Manual; Nicolet Magnetics Corporation: Freemont, CA, December 1982.
(37) Freeman, R.; Kempsell, S. P. *J. Magn. Reson.* **1980**, *38*, 453–479.
(38) Smith, J. M. *Chemical Engineering Kinetics*, 2nd ed.; McGraw-Hill: New York, 1970; pp 60–65.
(39) For a single filling of the drive syringes, each successive run required a slight increase in the amount of correction. The total correction never exceeded 10% during the time required to accumulate the desired number of repetitive runs. If solutions were allowed to remain in the drive syringes overnight, however, complete air oxidation of the reductant occurred.
(40) Lin, C.-T.; Rorabacher, D. B. *J. Phys. Chem.* **1974**, *78*, 305–308.

Table I. Physical Properties of Reagents Used in This Work for Electron-Transfer Kinetic Studies with $Cu^{II/I}([14]aneS_4)$ in Aqueous Solution at 25 °C, μ = 0.10 M (ClO_4^-)

reagent	E,[f] V	k_{22}, M^{-1} s^{-1}	$r \times 10^8$, cm[a]	log K_{12} (or K_{21})
$Cu([14]aneS_4)^{2+/+}$	0.59[b]		4.4[c]	0.00
reductants				
$Co(Me_4[14]tetraeneN_4)^{2+}$	0.562[d]	5.0×10^{-3}[e]	4.7[c]	0.47
$Ru(NH_3)_4bpy^{2+}$	0.526[f]	2.2×10^6[g]	4.4[c]	1.08
$Ru(NH_3)_5isn^{2+}$	0.387[h]	1.1×10^5[i]	3.8[i]	3.38
$Ru(NH_3)_5py^{2+}$	0.32[f]	1.1×10^5[g]	3.8[g]	4.57
oxidants				
$Ru(NH_3)_4bpy^{3+}$	0.526[f]	2.2×10^6[g]	4.4[c]	−1.08
$Ni([14]aneN_4)^{3+}$	0.95[j]	1.0×10^3[j]	3.6[j]	6.09
$Ru(NH_3)_2(bpy)_2^{3+}$	0.889[k]	8.4×10^7[g]	5.6[g]	5.06
$Fe(4,7\text{-}Me_2phen)_3^{3+}$	0.939[c]	3.3×10^8[l]	6.6[c]	5.90

[a] Effective radius in forming the outer-sphere complex preceding electron transfer (see ref 2). [b] Reference 24. [c] Reference 2. [d] Yee, E. L.; Cave, R. J.; Guyer, K. L.; Tyma, P. D.; Weaver, M. J. *J. Am. Chem. Soc.* **1979**, *101*, 1131–1137. Cf.: Endicott, J. F.; Durham, B.; Glick, M. D.; Anderson, T. J.; Kuszaj, J. M.; Schmonsees, W. G.; Balakrishnan, K. P. *J. Am. Chem. Soc.* **1981**, *103*, 1431–1440. [e] Corrected to μ = 0.10 M from the value determined in 1.0 M $HClO_4$: Durham, B. Ph.D. Dissertation, Wayne State University, 1977. [f] Yee, E. L.; Weaver, M. J. *Inorg. Chem.* **1980**, *19*, 1077–1079. [g] Reference 32. [h] Stanbury, D. M.; Haas, O.; Taube, H. *Inorg. Chem.* **1980**, *19*, 518–524. [i] The value of k_{22} is assumed to be identical to that for the corresponding pyridyl complex, $Ru(NH_3)_6py^{3+/2+}$. [j] Haines, R. I.; McAuley, A. *Coord. Chem. Rev.* **1981**, *39*, 77–119. McAuley, A.; Macartney, D. H.; Oswald, T. *J. Chem. Soc., Chem. Commun.* **1982**, 274–275. Fairbank, M. G.; Norman, P. R.; McAuley, A. *Inorg. Chem.* **1985**, *24*, 2639–2644. [k] Seddon, E. A.; Seddon, K. R. *The Chemistry of Ruthenium*; Elsevier: New York, 1984; p 444. [l] Ruff, I.; Zimonyi, M. *Electrochim. Acta* **1973**, *18*, 515–516.

be determined by the degree of linearity of plots of eq 9 using variable zero times. For some systems, the resultant selected zero time was at a point where the reaction was more than 50% complete. (In the accompanying supplementary material tabulating the experimental data, the extent of reaction which had occurred at the selected zero time is indicated both by the theoretical values of the initial reagent concentrations upon mixing and by the apparent concentration values at the selected zero time as determined from the absolute absorbance at that point.)

Cross Electron-Transfer Kinetic Studies. From earlier studies conducted in our laboratory,[2] we reported the results of kinetic measurements on the reduction of $Cu^{II}([14]aneS_4)$ using two reagents, $Co^{II}(Me_4[14]tetraeneN_4)(H_2O)_2$[42] and $Ru(NH_3)_4bpy$, and on the oxidation of $Cu^{I}([14]aneS_4)$ using $Fe^{III}(4,7\text{-}Me_2phen)_3$. In the current work, these studies have been greatly extended to include stopped-flow kinetic measurements on reactions involving the reduction of $Cu^{II}([14]aneS_4)$ with two additional reagents, $Ru^{II}(NH_3)_5bpy$ and $Ru^{II}(NH_3)_5isn$, and the oxidation of $Cu^{I}([14]aneS_4)$ with four reagents, $Ru^{III}(NH_3)_4bpy$, $Ru^{III}(NH_3)_2(bpy)_2$, $Ni^{III}([14]aneN_4)$, and $Fe^{III}(4,7\text{-}Me_2phen)_3$, the latter system having been repeated using the improved treatment accorded by eq 9. All cross reactions were carried out at 25 °C with an ionic strength of 0.10 M ($NaClO_4/HClO_4$), unless otherwise specified. The formal potentials and self-exchange rate constants, along with the effective ionic diameters, r, for all reagents used are given in Table I.

For each reaction system, three different series of reagent solutions were run using slightly varying initial concentrations of the reactants. For each series, at least six repetitive kinetic runs were made, each run being independently analyzed using eq 9 to generate an experimental value for k_{12} or k_{21} (see supplementary material). The cross reaction rate constant values for the individual runs within each series were then statistically averaged.

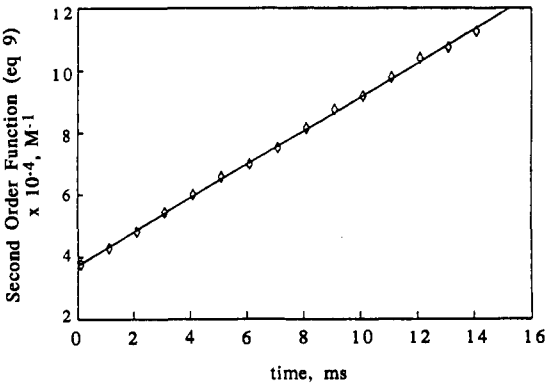

Figure 1. Plot of kinetic data for a single run involving the oxidation of $Cu^{I}([14]aneS_4)$ by $Fe^{III}(4,7\text{-}Me_2phen)_3$ in aqueous solution at 25 °C, μ = 0.10 M (CF_3SO_3H), utilizing eq 9. The point t = 0 represents the selected zero time. Initial concentrations upon mixing: $[Cu^{I}([14]aneS_4)]$ = 14.0 μM, $[Fe^{III}(4,7\text{-}Me_2phen)_3]$ = 24.5 μM, $[Cu^{II}([14]aneS_4)]$ = 0.6 μM. Extent of reaction at the selected zero time: X_0 = 8.17 μM. The cross-exchange rate constant, k_{21}, is obtained as the slope.

Table II. Experimental Cross Reaction Rate Constants and "Apparent" Work-Corrected Self-Exchange Rate Constants for $Cu^{II/I}([14]aneS_4)$ as a Function of the Potential Barrier Parameter in Aqueous Solution at 25 °C, μ = 0.1 M (ClO_4^- Except as Noted)

reagent	k_{12} (or k_{21}),[a] M^{-1} s^{-1}	app log k_{11} (cor)[b]	log $K_{12}k_{22}$ (or log $K_{21}k_{22}$)
reductants			
$Co([Me_4[14]tetraeneN_4)^{2+}$	7.5 (4)[c]	3.42	−1.83
$Ru(NH_3)_4bpy^{2+}$	4.80 (4) $\times 10^5$[c]	3.79	7.42
$Ru(NH_3)_5isn^{2+}$	1.9 (3) $\times 10^6$[d]	4.02	8.48
$Ru(NH_3)_5py^{2+}$	4.5 (3) $\times 10^6$	3.89	9.61
oxidants			
$Ru(NH_3)_4bpy^{3+}$	9.8 (3) $\times 10^4$[e]	2.58[f]	5.28
$Ni([14]aneN_4)^{3+}$	4.5 (4) $\times 10^5$	2.44[g]	9.09
$Ru(NH_3)_2bpy_2^{3+}$	2 (1) $\times 10^6$[h]	0.1	12.98
$Fe(4,7\text{-}Me_2phen)_3^{3+}$	5.2 (3) $\times 10^6$[e]	−0.38	14.42
	6.6 (3) $\times 10^6$[c,i]	−0.17	
	9.9 (3) $\times 10^6$[c,i]	0.20	
NMR self-exchange		3.81, 3.94	

[a] Values in parentheses in this and subsequent tables represent the standard deviation for the last digit listed: e.g., 4.80 (4) $\times 10^5$ represents (4.80 ± 0.04) $\times 10^5$. [b] Apparent self-exchange rate constants include corrections for the work term and the nonlinear term. [c] Reference 2. [d] Rate constant obtained at 23.6 °C. [e] Ionic strength controlled with 0.10 M $HNO_3/NaNO_3$. [f] Obtained under second-order conditions with both reactants present at concentration levels of 54–120 μM (cf. Table III). [g] Obtained under second-order conditions with both reactants present at concentration levels of 9–23 μM (cf. Table III). [h] Second-order rate constant corrected to μ = 0.10 M (from data at μ = 0.15 M). [i] Ionic strength controlled with 0.10 M CF_3SO_3H.

On the basis of the stepwise rate constants for the conformational changes in Scheme I, as evaluated from the electrochemical measurements,[24] it appeared that the reactions involving $Ni^{III}([14]aneN_4)$ and $Ru^{III}(NH_3)_4bpy$ as oxidants might involve a switch to conformationally-limited kinetic behavior (see Discussion). Thus, to provide a more extensive evaluation of this system, the concentration of the Ni(III) reagent was varied over a

(41) The derivation of a modified form of eq 9, incorporating the treatment of the cell concentration gradient, has been solved by approximate methods and will be presented elsewhere: Meagher, N. E.; Rorabacher, D. B. To be submitted for publication.

(42) The reagent $Co^{II}(Me_4[14]tetraeneN_4)(H_2O)_2$, often represented in this paper without the coordinated water molecules, is diaquo(2,3,9,10-tetramethyl-1,4,8,11-tetraazacyclotetradeca-1,3,8,10-tetraene)cobalt(II) ion, also known as Co^{II}(TIM) (ref 2).

Table III. Experimental Cross Reaction Rate Constants for the Oxidation of $Cu^{I}([14]aneS_4)$ with $Ni^{III}([14]aneN_4)$ and $Ru^{III}(NH_3)_4bpy$ as a Function of Reagent Concentration in Aqueous Solution at 25 °C, μ = 0.10

init oxidant concn, mM	$k_{21} \times 10^{-4}$, M^{-1} s^{-1} [a]	app log $k_{11(ox)}$ (cor)[b]	init oxidant concn, mM	$k_{21} \times 10^{-4}$, M^{-1} s^{-1} [a]	app log $k_{11(ox)}$ (cor)[b]
		$Ni^{III}([14]aneN_4)$			
series I[c]			series II[c]		
0.0080[d]	93	3.15	0.50	7.2	0.92
0.0120[d]	107	3.28	1.00	5.6	0.62
0.0181[d]	62, 54, 35, 32	2.8, 2.7, 2.3, 2.2	2.00	3.2	0.12
0.036[d]	10.0	1.14	4.0[e]	4.6	0.44
0.072[d]	13.5	1.41	8.0[e]	1.44	−0.60
0.145	49	2.51			
0.290	24	1.87	series III[c]		
0.67	8.5	0.94	0.050[d]	17.3	1.62
0.78	10	1.12	0.100[d]	16.8	1.58
0.89	11	1.21	0.50	4.9	0.48
1.00	7.3	0.86	1.00	3.8	0.25
1.11	6.9	0.81	2.00	1.8	−0.38
1.16	5.3	0.56	4.0[e]	2.1	−0.25
1.22	6.0	0.68	8.0[e]	1.2	−0.78
1.33	5.0	0.53			
		$Ru^{III}(NH_3)_4bpy$			
0.555[f]	1.33	2.84	1.11[f]	0.64	2.21
1.00[g]	1.46	2.92	1.11[g]	1.35	2.84
1.11[c]	0.67	2.24	2.00[g]	0.168	1.12

[a] For $[Ni^{III}([14]aneN_4)] > 0.1$ mM, the kinetic data were analyzed as pseudo first order; the apparent second-order rate constants listed were then calculated as $k_{21} = k'/[A_{ox}]$. [b] Self-exchange rate constants include corrections for the work term and the nonlinear term. [c] $[Cu^{I}L] = 0.0111$ mM. [d] Data omitted from plot in Figure 7 as $[Ni^{III}([14]aneN_4)]$ varied during reaction. [e] Data omitted from plot in Figure 7 due to apparent contribution from pathway B. [f] $[Cu^{I}L] = 0.0250$ mM. [g] $[Cu^{I}L] = 0.122$ mM.

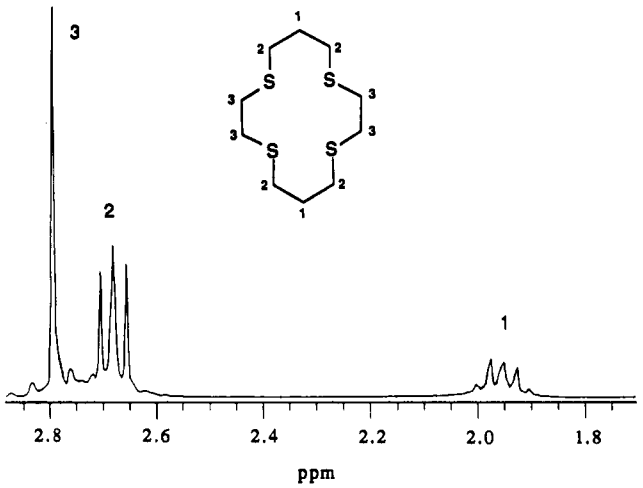

Figure 2. ^1H NMR spectrum of $[14]aneS_4$ in $CDCl_3$.

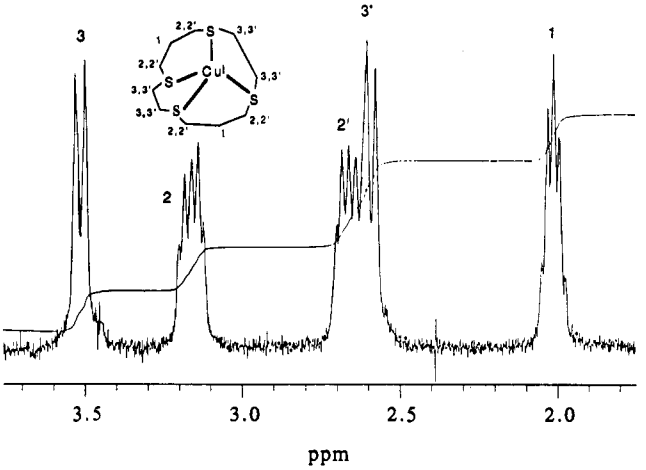

Figure 3. ^1H NMR spectrum of $Cu^{I}([14]aneS_4)$ in D_2O.

1000-fold range (8 μM to 8 mM). Kinetic runs involving large excesses of Ni(III) were analyzed as pseudo-first-order processes. Similar attempts to vary $[Ru^{III}(NH_3)_4bpy]$ over an extended range proved infeasible.[43] The results of these concentration studies are tabulated in Table III.

Self-Exchange Electron-Transfer Studies via NMR. The self-exchange rate constant for $Cu^{II/I}([14]aneS_4)$, $k_{11(ex)}$, as defined by reaction 2, was determined independently from ^1H NMR line-broadening measurements using the same approach recently described for a related Cu(II)/(I) macrocyclic pentathiaether system.[44] The peaks in the ^1H spectrum for the free ligand in $CDCl_3$ (Figure 2) and for the $Cu^{I}L$ complex in D_2O (Figure 3) have been assigned from decoupling experiments. The principal line-broadening measurements were made utilizing the doublet furthest downfield (≈3.5 ppm) in the $Cu^{I}L$ spectrum (designated as 3 in Figure 3), which was assigned to protons on the ethylene bridging groups. In evaluating the data, it was necessary to deconvolute this doublet into its constituent peaks.[45] A check was made on the validity of these data by repeating the analysis of the line-broadening using the pair of overlapping triplets centered at approximately 3.15 ppm (designated as 2 in Figure 3), which were assigned to the protons on the α carbons of the trimethylene bridges. This approach yielded similar results, although the increased complexities involved in deconvoluting the pair of triplets decreased the precision of the data.

Upon addition of measured quantities of $Cu^{II}L$ to a solution containing $Cu^{I}L$, the doublet and the pair of triplets were observed to broaden in a manner consistent with the interconversion of diamagnetic and paramagnetic species, and the data were fitted to the expression of McConnell and Berger[46,47] as derived from the Block equations,

$$k_{11} = \frac{1}{[P]}\left[\left(\frac{1}{T_2}\right)_{DP} - \left(\frac{1}{T_2}\right)_{D}\right] \qquad (10)$$

(43) The reaction of $Ru^{III}(NH_3)_4bpy$ with $Cu^{I}([14]aneS_4)$ is thermodynamically unfavorable. Thus, a large excess of the Ru(III) reagent is required to produce a significant reaction. This severely limits the concentration range accessible for study.

(44) Vande Linde, A. M. Q.; Juntunen, K. L.; Mols, O.; Ksebati, M. B.; Ochrymowycz, L. A.; Rorabacher, D. B. *Inorg. Chem.* **1991**, *30*, 5037–5042.

(45) In deconvoluting the selected doublet, improved precision was obtained by establishing the requirement that the two constituent peaks be identifical in height and breadth (despite the skewing of the doublet due to coupling).

(46) McConnell, H. M.; Berger, S. B. *J. Chem. Phys.* **1957**, *27*, 230–234.

(47) Gutowsky, H. S.; McCall, D. W.; Slichter, C. P. *J. Chem. Phys.* **1953**, *21*, 279–292.

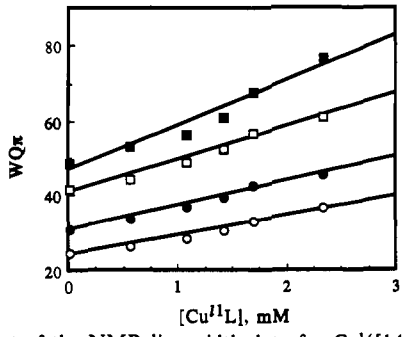

Figure 4. Plot of the NMR line-width data for $Cu^{I}([14]aneS_4)$ as a function of $[Cu^{II}([14]aneS_4)]$ according to eq 11 for 5 (○), 15 (●), 25 (□), and 35 °C (■). The self-exchange rate constant, $k_{11(ex)}$, for each temperature is obtained as the slope.

where [P] is the concentration of the added paramagnetic species (i.e., the molar concentration of $Cu^{II}L$), $(T_2)_D$ is the transverse relaxation time of the selected ^1H for a solution containing only the diamagnetic species (i.e., $Cu^{I}L$), and $(T_2)_{DP}$ is the corresponding quantity for a solution containing both the diamagnetic and paramagnetic species. It was determined that all of the appropriate conditions for applying eq 10 were met.[48] For calculating the value of $k_{11(ex)}$, the relationship of the transverse relaxation time to the peak width (i.e., $T_2^{-1} = \pi W_{1/2}$) was substituted into eq 10, which was then rearranged to the form

$$W_{DP}\mathcal{Q}\pi = W_D\mathcal{Q}\pi + k_{11(ex)}[Cu^{II}L] \qquad (11)$$

where W_{DP} is the peak width at half-height of a single proton resonance peak from a solution containing both the diamagnetic ($Cu^{I}L$) and paramagnetic ($Cu^{II}L$) species, W_D is the corresponding value for a solution containing only the diamagnetic species, and $\mathcal{Q}$ is a factor used to correct the extent of outer-sphere complex formation at the specific ionic strength used (represented by the outer-sphere equilibrium constant $K_{OS(s)}$) to a common ionic strength value of 0.10 M (represented by the constant $K_{OS(0.1)}$) as previously described:[44]

$$\mathcal{Q} = K_{OS(0.1)}/K_{OS(s)} \qquad (12)$$

The extent of line-broadening caused by the paramagnetic Cu(II) ion, independent of electron exchange, was determined by preparing a series of solutions containing only $Cu^{I}L$ and Cu^{II}_{aq} (in the form of $Cu(NO_3)_2$) in D_2O, the concentration of the latter species being varied up to 0.10 M.[49] These measurements showed that considerable broadening occurred due to the paramagnetic ion at the higher concentration level, but the influence was not experimentally significant in the concentration range of the added $Cu^{II}L$ species. However, in view of the low stability of the $Cu^{II}L$ species,[34] a large amount of Cu^{II}_{aq} (0.05 M) was added to all solutions to minimize the dissociation of the divalent complex. This resulted in a uniform broadening of the $Cu^{I}L$ peaks but did not otherwise affect the data resolution.

Within a single series of determinations, the same set of solutions was utilized in obtaining line-broadening measurements at 5, 15, 25, and 35 °C. Concentration changes resulting from thermal expansion of the solvent were not significant relative to the achievable level of data reproducibility, and no corrections were made for this phenomenon. After optimal conditions for the NMR measurements were determined, two separate series of solutions were prepared and used for the final measurements. The data from one series are plotted in Figure 4 using eq 11. The resulting $k_{11(ex)}$ values for both series of measurements, obtained by linear least-squares analysis as the calculated slope, are tabulated in Table IV, yielding a mean value of log $k_{11(ex)}$ = 3.88 ± 0.09 at 25 °C.

Table IV. Self-Exchange Rate Constant Values Determined from NMR Line-Broadening Measurements on $Cu^{II/I}([14]aneS_4)$ as a Function of Temperature in Aqueous Solution, Corrected to μ = 0.10 M (NO_3^-)

	$k_{11} \times 10^{-3}$, M^{-1} s^{-1}	
T, °C	series I,[a,b] pD = 4.38	series II,[a,c] pD = 3.02
5	3.1 (3)	5.2 (5)
15	4.5 (5)	6.5 (4)
25	6.4 (7)	8.8 (6)
35	9.5 (5)	12.1 (14)

Activation Parameters

	series I[a,b]	series II[a,c]	mean
ΔH^*, kJ mol^{-1}	23.9 (10)	17.5 (2)	20.7 ± 4.5
ΔS^*, J K^{-1} mol^{-1}	−92 (3)	−110 (1)	−101 ± 13

[a] Values in parentheses represent the standard deviation for the last digit(s) listed. [b] Series I: $[Cu^{I}L]$ = 0.370 mM; $[Cu^{II}L]_{max}$ = 4.01 mM; $[Cu^{II}_{aq}]$ = 51 mM. [c] Series II: $[Cu^{I}L]$ = 0.388 mM; $[Cu^{II}L]_{max}$ = 2.33 mM; $[Cu^{II}_{aq}]$ = 54 mM.

In determining the activation parameters for the self-exchange rate constant, the variable temperature data were plotted according to the Arrhenius equation in the form

$$\ln k_{11(ex)} = \ln A - E_a/RT \qquad (13)$$

where A is the Arrhenius frequency factor, E_a is the activation energy, R is the universal gas constant, and T is the absolute temperature. The values of ΔH^* and ΔS^* were then calculated according to the following relationships (for reactions in solution):[50]

$$\Delta H^* = E_a - RT + P\Delta V^* \approx E_a - 2.5 \text{ kJ mol}^{-1} \qquad (14)$$

$$\Delta S^* = R[\ln k_{11(ex)} - \ln (k_BT/h)] + \Delta H^*/T \qquad (15)$$

where k_B represents the Boltzmann constant and h represents Planck's constant. The resulting activation parameters calculated for the two series of measurements are included in Table IV.

Discussion

Resolution of Self-Exchange Rate Constants. The applicability of the Marcus relationship to electron-transfer reactions involving Cu(II)/(I) systems has been called into question previously as a result of apparent inconsistencies in literature data on oxidation and reduction measurements.[51,52] For the current study, the availability of electrochemical evaluations of the rate constants for conformational interconversion,[24] the direct determination of the $Cu^{II/I}([14]aneS_4)$ self-exchange rate constant via NMR line-broadening measurements, and the measurement of cross reaction kinetics for both $Cu^{II}L$ reduction and $Cu^{I}L$ oxidation with a number of counterreagents make it possible to test the veracity of the Marcus approach in a more thorough manner than has been possible previously. As is demonstrated below, the data also permit us to examine the conformance of the kinetic behavior to that predicted by the proposed mechanism depicted in Scheme I.

As applied to reaction 1, the Marcus relationship can be expressed in the form[6]

$$k_{12} = (k_{11}k_{22}K_{12}f_{12})^{1/2}W_{12} \qquad (16)$$

where k_{11} and k_{22} are the self-exchange rate constants for the

(48) The conditions required for eq 10 include the following: $(T_2)_D \geq \tau_D \gg \tau_P \gg \tau_p$ and $(\delta\omega\ \tau_P/2)^2 \gg 1$, where τ_D and τ_P are the mean lifetimes of the diamagnetic and paramagnetic species, respectively, following electron transfer; τ_p is the paramagnetic spin–lattice relaxation time; $\delta\omega$ is the hyperfine splitting of the electron resonance of the paramagnetic species due to the proton; and $(T_2)_D$ is the spin–spin relaxation time of the diamagnetic species (cf. ref 44).

(49) In the absence of hydroxide bridging, the self-exchange rate constant for $Cu_{aq}^{2+/+}$ has been found to be approximately 2.5×10^{-6} M^{-1} s^{-1} at 25 °C (Martin, M. J. Ph.D. Dissertation, Wayne State University, 1980). In the current experiments, strongly acidic solutions were used to avoid possible hydroxide bridge formation. In conjunction with the much lower potential value for the $Cu_{aq}^{2+/+}$ redox couple relative to $Cu^{II/I}L$, the contribution of electron transfer involving $Cu^{I}L$ and Cu_{aq}^{2+} was negligible.

(50) Steinfeld, J. I.; Francisco, J. S.; Hase, W. L. *Chemical Kinetics and Dynamics*; Prentice-Hall: Englewood Cliffs, NJ, 1989; pp 322–323. The $P\Delta V^*$ term in eq 14 is negligible for reactions in solution.

(51) Lee, C.-W.; Anson, F. C. *J. Phys. Chem.* **1983**, *87*, 3360–3362.

(52) Lee, C. W.; Shin, D. S.; Chair, T. S.; Kim, K. *Bull. Korean Chem. Soc.* **1991**, *12*, 454–455.

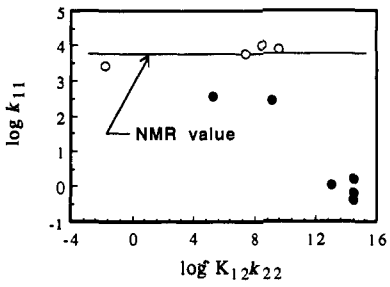

Figure 5. Plot of the logarithmic values of the *apparent* self-exchange rate constant for $Cu^{II/I}([14]aneS_4)$, as calculated from the Marcus cross relationship, as a function of the "potential barrier parameter," log $K_{12}k_{22}$, for the cross reactions included in this study. The open circles represent apparent $k_{11(red)}$ values, while the solid circles represent $k_{11(ox)}$ values.

$Cu^{II/I}L$ and $A_{ox/red}$ redox couples, respectively, K_{12} is the equilibrium constant for reaction 1, f_{12} represents a nonlinear correction term, and W_{12} is the work term (i.e., electrostatic correction term).[2,6] A corresponding expression can be written for the reverse reaction rate constant, k_{21}. Since the value of K_{12} (or K_{21}) is dependent upon the potential of the two constituent redox couples,

$$\ln K_{12} = (E_1^f - E_2^f)n\mathcal{F}/RT \qquad (17)$$

an increase in either the reaction potential or the self-exchange rate constant of the selected counterreagent, k_{22}, should result in an increase in the overall reaction rate constant.

On the basis of the E^f and k_{22} (as well as r) values listed for each reagent in Table I, we have utilized eq 16 to calculate the apparent (work term corrected) self-exchange rate constant value for the $Cu^{II/I}([14]aneS_4)$ redox couple from the kinetic data obtained for each of the cross reactions studied in this work under second-order conditions.[2] The resultant values, applicable to reactions at 25 °C and 0.10 M ionic strength, are listed in logarithmic form in the third column of Table II. The values of log $K_{12}k_{22}$ (or log $K_{21}k_{22}$ for $Cu^{I}L$ oxidation reactions), which we have termed the "potential barrier parameter" (eq 16), are included in the right-hand column as an indicator of the intrinsic rate velocity anticipated for each reaction system. Also listed at the bottom of this table for comparison are the corresponding log $k_{11(ex)}$ values obtained directly from NMR line-broadening.

As emphasized in Figure 5, it is apparent that the application of the Marcus relationship to all four cross reactions involving $Cu^{II}([14]aneS_4)$ *reduction* yields $k_{11(red)}$ values which are in excellent agreement with the NMR $k_{11(ex)}$ value. In fact, the level of agreement among these values is remarkably consistent considering the fact that the "potential barrier parameter" for the reductants utilized covers 11 orders of magnitude (Table II). From this we conclude that the Marcus relationship is directly applicable to electron-transfer reactions involving the *reduction* of this copper complex.

By contrast, the values obtained for $k_{11(ox)}$ are as much as 4 orders of magnitude smaller than $k_{11(ex)}$. Moreover, the data in Figure 5 imply that $k_{11(ox)}$ decreases as log $K_{21}k_{22}$ increases. This observation suggests that the various oxidation reactions may have been carried out under conditions where the conformational change associated with R → P (designated by rate constant k_{RP} in Scheme I) has become (or is becoming) rate-limiting. In fact, with the availability of the estimates for the various stepwise rate constants in Scheme I, as generated in our related electrochemical study,[24] we are now in a position to test the validity of this suggestion.

Examination of Square Scheme Behavior. In terms of the mechanism depicted in Scheme I, complete differential kinetic expressions for the reduction of $Cu^{II}L$ and the oxidation of $Cu^{I}L$ can be derived using the steady-state approximation for the metastable intermediates (P and Q). In carrying out this derivation, we have assumed that $Cu^{II}L$ and $Cu^{I}L$ exist primarily in the form of the stable conformers, O and R (as confirmed by our independent electrochemical evidence),[24] and we have included the contributions of back electron transfer preceding conformational rearrangement, i.e., Q + A_{red} → R for oxidation reactions and P → O + A_{ox} for reduction reactions. The resulting complete expressions for reduction and oxidation via Scheme I are

Reduction:

$$-\frac{d[Cu^{II}L]}{dt} = \left(\frac{k_{A2}k_{PR}}{k_{2A}[A_{ox}] + k_{PR}} + \frac{k_{B2}k_{OQ}}{k_{B2}[A_{red}] + k_{QO}}\right)[O][A_{red}] \qquad (18)$$

Oxidation:

$$-\frac{d[Cu^{I}L]}{dt} = \left(\frac{k_{2A}k_{RP}}{k_{2A}[A_{ox}] + k_{PR}} + \frac{k_{2B}k_{QO}}{k_{B2}[A_{red}] + k_{QO}}\right)[R][A_{ox}] \qquad (19)$$

In each expression, the first and second parenthetical terms represent the kinetic contributions of pathways A and B, respectively. Depending upon which parenthetical term is dominant (i.e., whether pathway A or B is more favorable) and the relative magnitude of the two terms in the denominator of each of the two parenthetical terms, a number of limiting expressions may result. However, since the voltammetric data in our related electrochemical study[24] clearly indicate that intermediate P is intrinsically more stable than intermediate Q, only the limiting conditions associated with pathway A are considered below:

Reduction:

Pathway A dominant:

$$\left(\frac{k_{A2}k_{PR}}{k_{2A}[A_{ox}] + k_{PR}}\right) \gg \left(\frac{k_{B2}k_{OQ}}{k_{B2}[A_{red}] + k_{QO}}\right)$$

If $k_{2A}[A_{ox}] \ll k_{PR}$: $$-\frac{d[Cu^{II}L]}{dt} = k_{A2}[O][A_{red}] \qquad (18a)$$

If $k_{2A}[A_{ox}] \gg k_{PR}$: $$-\frac{d[Cu^{II}L]}{dt} = K_{A2}k_{PR}\frac{[O][A_{red}]}{[A_{ox}]} \qquad (18b)$$

Oxidation:

Pathway A dominant:

$$\left(\frac{k_{2A}k_{RP}}{k_{2A}[A_{ox}] + k_{PR}}\right) \gg \left(\frac{k_{2B}k_{QO}}{k_{B2}[A_{red}] + k_{QO}}\right)$$

If $k_{2A}[A_{ox}] \ll k_{PR}$: $$-\frac{d[Cu^{I}L]}{dt} = K_{PR}^{-1}k_{2A}[R][A_{ox}] \qquad (19a)$$

If $k_{2A}[A_{ox}] \gg k_{PR}$: $$-\frac{d[Cu^{I}L]}{dt} = k_{RP}[R] \qquad (19b)$$

Of these expressions, eqs 18a and 19a represent the situation in which P and R are fully equilibrated, leading to normal Marcus behavior. Under this condition, the existence of intermediates is not apparent in the kinetic data since they are at all times in equilibrium with the stable conformers. By contrast, eqs 18b and 19b represent the condition where the P ⇌ R conformational interconversion is the rate-limiting step, resulting in "gated" electron-transfer behavior.

Since Marcus theory appears to be applicable to all reduction reactions included in this study, the values of $k_{11(red)}$ must represent the equilibrated condition where the rate-determining step involves the O,P redox couple. Thus, we presume that the value of the self-exchange rate constant for this specific redox couple, designated as k_{AA}, may be calculated as follows, using the value of K_{PR} estimated in our electrochemical study:[24]

$$O^* + P \rightleftharpoons P^* + O \qquad k_{AA}$$

$$k_{AA} = k_{11(ex)}K_{PR} \approx (7.6 \times 10^3)(50) \approx 4 \times 10^5\ M^{-1}\ s^{-1} \qquad (20)$$

Demonstration of Gated Behavior. As noted above in generating eqs 19a and 19b, the relative magnitudes of k_{PR} and $k_{2A}[A_{ox}]$ determine which limiting expression pertains for reaction systems in which pathway A is dominant. Of these terms, k_{PR} is a fixed quantity while k_{2A} depends upon the values of K_{12} and k_{22}. Thus, with appropriate variations in the reaction potential and/or the

Table V. Estimated "Critical" (Threshold) Concentrations for the Various Counterreagents Studied Which Are Predicted To Generate Gated Electron-Transfer Behavior in Cross Reactions with $Cu^{II/I}([14]aneS_4)$

reagent	est K_{2A}[a]	est k_{2A}, M^{-1} s^{-1} [a]	crit value for $[A_{ox}]$, M[b]
reductants			
$Co(Me_4[14]tetraeneN_4)^{2+}$	0.25	20	1×10^2
$Ru(NH_3)_5py^{2+}$	2×10^{-2}	3×10^4	0.1
$Ru(NH_3)_5isn^{2+}$	1×10^{-3}	3×10^4	0.5
$Ru(NH_3)_4bpy^{2+}$	4	2×10^6	1.5×10^{-3}
oxidants			
$Ru(NH_3)_4bpy^{3+}$	4	2×10^6	1.5×10^{-3}
$Ni([14]aneN_4)^{3+}$	6×10^7	2×10^8	1.5×10^{-5}
$Ru(NH_3)_2bpy_2^{3+}$	6×10^6	1×10^{10}	3×10^{-7}
$Fe(4,7\text{-}Me_2phen)_3^{3+}$	4×10^7	7×10^{10}	4×10^{-8}

[a] For values used in calculation, see ref 53. [b] The critical value of $[A_{ox}]$ indicates the concentration level at which $k_{2A}[A_{ox}]$ becomes equal to k_{PR} ($\approx 3 \times 10^3$ s^{-1}) in eqs 18 and 19.

self-exchange rate constant of the counterreagent (the two terms comprising the "potential barrier parameter"), or in the concentration of the oxidant, $[A_{ox}]$, the limiting condition for eq 19b should eventually be met and "gated" electron transfer should be observed.

Utilizing the data obtained from our related electrochemical study,[24] along with the appropriate parameters for each counterreagent used in our cross reaction studies (Table I), we have calculated the value of $[A_{ox}]$ which would bring about the transitional condition, $k_{PR} \approx k_{2A}[A_{ox}]$ (i.e., $[A_{ox}] = k_{PR}/k_{2A}$).[53] As listed in Table V, these "critical" values of $[A_{ox}]$ range from 0.1 to 100 M for three of the *reductants* utilized, greatly exceeding the concentration levels used in our kinetic studies. In the case of the fourth *reductant*, $Ru^{II}(NH_3)_4bpy$, the critical concentration is only 10^{-3} M, but this is also considerably larger than the concentrations used in our reduction studies. Therefore, we conclude that eq 18a should apply to the kinetic measurements for all *reduction* studies which have been conducted with $Cu^{II}([14]aneS_4)$, and *normal Marcus behavior should apply*. This is consistent with the close agreement of all $k_{11(red)}$ values with $k_{11(ex)}$ as noted above.

For the two strongest *oxidizing* agents, $Ru^{III}(NH_3)_2(bpy)_2$ and $Fe^{III}(4,7\text{-}Me_2phen)_3$, the critical values of $[A_{ox}]$ are well below 10^{-6} M. Thus, the kinetic studies on these latter reactions were carried out under conditions where conformational gating occurs, presumably accounting for the very small "apparent" values of $k_{11(ox)}$ (Table II). For the two intermediate *oxidizing* agents, $Ru^{III}(NH_3)_4bpy$ and $Ni^{III}([14]aneN_4)$, the critical concentrations are calculated to be about 10^{-3} and 10^{-5} M, respectively, almost exactly the concentration levels used in our initial oxidation studies as tabulated in Table II. Thus, *the oxidation kinetic measurements conducted with these two reagents should be in the transitional range between eqs 19a and 19b.*

In striving to bridge the transition from nongated to gated conditions, we attempted kinetic measurements with these latter two oxidants over a wide concentration range. In the case of $Ru^{III}(NH_3)_4bpy$, this attempt proved unsuccessful since large concentrations of the latter reagent are required to drive the oxidation reaction thermodynamically uphill, and solubility limits do not permit a significant concentration range to be observed. For $Ni^{III}([14]aneN_4)$, however, it proved possible to vary the reagent concentration 1000-fold (Table III).

The apparent second-order rate constant (k_{21}) values listed in Table III have been used to calculate "apparent" $k_{11(ox)}$ values (with work term corrections) using eq 16. The results are plotted in logarithmic form in Figure 6 as a function of the reagent concentration, $[Ni^{III}([14]aneN_4)]$. This plot clearly shows that

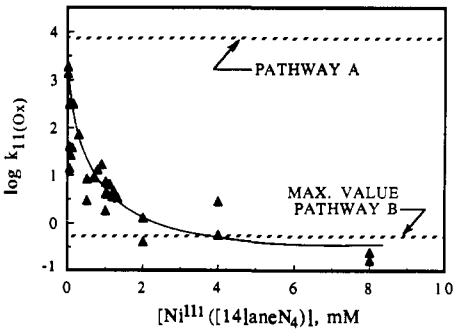

Figure 6. Plot of the *apparent* logarithmic self-exchange rate constant for $Cu^{II/I}([14]aneS_4)$, $k_{11(ox)}$, as a function of the concentration of the oxidizing agent, $Ni^{III}([14]aneN_4)$. For reactions following a single pathway, a constant value of $k_{11(ox)}$ should be obtained corresponding either to the value marked for pathway A or to that marked for pathway B. The data shown appear to be in transition between these two pathways. (The curve shown has no theoretical significance.)

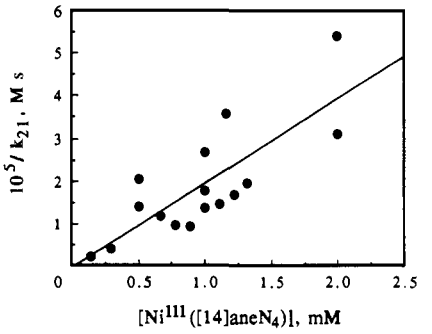

Figure 7. Plot of eq 21a for the oxidation of $Cu^{I}([14]aneS_4)$ by $Ni^{III}([14]aneN_4)$ in aqueous solution at 25 °C. Kinetic data obtained under conditions where $Ni^{III}([14]aneN_4)$ was present in less than 10-fold excess have been omitted since the reagent concentration could not be considered constant throughout the reaction. The reciprocal slope yields $k_{RP} = 50$ (± 10) s^{-1} for the controlling conformational conversion R → P. The intercept, representing the value anticipated for pathway A under equilibrated conditions (i.e., $1/k_{21} = K_{PR}/k_{2A}$), is not statistically different from zero on the plot shown. This is in accord with the theoretical intercept calculated as $1/k_{21} = (k_{11(ex)}k_{22}K_{21}f_{21})^{-1/2}(W_{21})^{-1} = 4.6 \times 10^{-7}$ M s (cf. ref 53).

the highest values of the "apparent" $k_{11(ox)}$ are approaching the value expected for pathway A as represented by $k_{11(ex)}$ determined directly from the NMR self-exchange studies. From this observation we conclude that, at very low Ni(III) concentrations, kinetic behavior characteristic of pathway A is dominant. At the high [Ni(III)] limit in Figure 6, the apparent $k_{11(ox)}$ values are approaching the $k_{11(ox)}$ values obtained with the strongest oxidants tested, $Ru^{III}(NH_3)_2(bpy)_2$ and $Fe^{III}(4,7\text{-}Me_2phen)_3$. Thus, changing the concentration of $Ni^{III}([14]aneN_4)$ appears to bridge the behavior observed with the reduction kinetic studies and the oxidations using $Ru^{III}(NH_3)_2(bpy)_2$ and $Fe^{III}(4,7\text{-}Me_2phen)_3$ as noted earlier in Figure 5.

On the basis of the assumption that both of the terms representing pathway A in eq 18 are contributing to the observed kinetics in the oxidation of $Cu^{I}([14]aneS_4)$ by $Ni^{III}([14]aneN_4)$, i.e.,

$$k_{21} = \frac{k_{2A}k_{RP}}{k_{2A}[A_{ox}] + k_{PR}} \tag{21}$$

we have plotted the reciprocal form of this expression to separate the variables and generate the following linear relationship:

$$\frac{1}{k_{21}} = \frac{[A_{ox}]}{k_{RP}} + \frac{K_{PR}}{k_{2A}} \tag{21a}$$

In Figure 7, the data from Table III are plotted according to eq 21a. For the solid points, covering a 14-fold concentration range for the counterreagent, the reciprocal slope yields $k_{RP} = 50$ (± 10) s^{-1}. This is in surprisingly good agreement with the previous

(53) The value of k_{2A} has been calculated using eq 16 in the form $k_{2A} = (k_{AA}k_{22}K_{2A}f_{2A})^{1/2}W_{2A}$, where $k_{AA} = 4 \times 10^5$ M^{-1} s^{-1} (eq 20). The value of K_{2A} is calculated using the potential for the O_2P redox couple, estimated to be ca. 0.49 V in aqueous solution based on $E_{OR}' = 0.59$ V and $K_{PR} \approx 50$. For k_{PR}, a value of 3×10^3 s^{-1} has been utilized (see ref 24).

estimate of $k_{RP} \approx 60\ s^{-1}$ obtained in 80% methanol at 25 °C (based on our rapid-scan cyclic voltammetric measurements).[24] *Thus, we have generated definitive evidence for the existence of gated electron-transfer behavior in a Cu(II)/(I) system which is controlled by conformational change.*

Limiting Parameters for Pathway B. The data for the two highest [Ni(III)] values (4 and 8 mM) in Table III were omitted from the plot in Figure 7, as it is suspected that the kinetics observed may represent a transition to pathway B. Consideration of the square scheme mechanism indicates that, once conformationally-gated electron-transfer behavior has been achieved, further increases in the "potential barrier parameter" for oxidation reactions, or in the concentration of the oxidant, A_{ox}, should eventually cause the value of k_{2B} (i.e., the electron-transfer step in pathway B) to increase until the rate of oxidation via pathway B exceeds the conformationally-limited rate by pathway A. At that point a switch in the reaction pathway should occur; that is, the second parenthetical term in eq 19 will become dominant, for which there are, once again, two limiting cases:

Oxidation

Pathway B dominant:

$$\left(\frac{k_{2A}k_{RP}}{k_{2A}[A_{ox}] + k_{PR}}\right) \ll \left(\frac{k_{2B}k_{QO}}{k_{B2}[A_{red}] + k_{QO}}\right)$$

If $k_{B2}[A_{red}] \ll k_{QO}$: $$-\frac{d[Cu^{I}L]}{dt} = k_{2B}[R][A_{ox}] \qquad (19c)$$

If $k_{B2}[A_R] \gg k_{QO}$: $$-\frac{d[Cu^{I}L]}{dt} = K_{B2}^{-1}k_{QO}\frac{[R][A_{ox}]}{[A_{red}]} \qquad (19d)$$

Of these two limiting expressions, the conditions for eq 19c will prevail for thermodynamically favorable reactions[11] and regular second-order behavior will again be observed. Normal Marcus behavior should apply to such reactions except that the characteristic self-exchange rate constant for $Cu^{II/I}([14]aneS_4)$ will be altered to that representative of pathway B.

It is unclear whether the observed second-order rate constants obtained using $Ru^{III}(NH_3)_2(bpy)_2$ and $Fe^{III}(4,7\text{-}Me_2phen)_3$ as oxidants are still within the region of conformational control or whether they represent pathway B. At the very least, however, it is obvious that oxidation via pathway B *cannot be faster* than the kinetics observed with these latter reagents. Thus, the calculated $k_{11(ox)}$ values obtained from these reactions can be assumed to represent an *upper limit* for the self-exchange rate constant characteristic of pathway B, $k_{11(B)}$, from which we can then estimate the maximum specific self-exchange rate constant for the $Cu^{II}L(Q)/Cu^{I}L(R)$ redox couple, k_{BB}, as follows:

$$Q^* + R \rightleftharpoons R^* + Q \qquad k_{BB}$$

$$k_{BB} \le k_{11(ox)}/K_{OQ} \approx 1/(4 \times 10^{-5}) \approx 3 \times 10^4\ M^{-1}\ s^{-1} \qquad (22)$$

This estimate for the *maximum* value of k_{BB} is very nearly identical to the previous estimate of $k_{BB} \approx 7 \times 10^4\ M^{-1}\ s^{-1}$ based on our electrochemical study.[24] *Therefore, we conclude that the kinetic data for the oxidation of $Cu^{I}([14]aneS_4)$ by $Ru^{III}(NH_3)_2(bpy)_2$ and $Fe^{III}(4,7\text{-}Me_2phen)_3$ probably represent reaction via pathway B.*

Despite the change in mechanistic behavior for the oxidation reactions included in this study (from eq 19a to eq 19b and, ultimately, to eq 19c), no similar shift in behavior (e.g., from eq 18a to eq 18b) is expected for the reduction reactions. As noted in Table V, the calculated critical values of $[A_{ox}]$ are exceptionally large for reactions involving thermodynamically favorable reducing agents and would not be exceeded in normal practice. Brunschwig and Sutin[11] have already made note of the fact that gated behavior will normally be observed *only in one direction* for systems conforming to Scheme I. Thus, all *reduction* reactions included in this study should conform to eq 18a as has been assumed.

Conclusions. The previously noted discrepancies in the $Cu^{II}L/Cu^{I}L$ self-exchange rate constants, as calculated for Cu(II) reductions ($k_{11(red)}$) and Cu(I) oxidations ($k_{11(ox)}$), are shown to arise from gated electron-transfer behavior in which the oxidation reactions are limited by the rate constant for conformational change in converting the thermodynamically stable form of $Cu^{I}L$ (designated as R) to a metastable intermediate (P) prior to the actual electron-transfer step. The point at which this change in oxidation behavior occurs has been shown to be in excellent agreement with predictions based on the estimated rate constant for this conformational change ($k_{RP} \approx 60\ s^{-1}$), as evaluated from rapid-scan cyclic voltammetry. Ultimately, the oxidation reactions switch to the alternate pathway (pathway B) as the rate for this latter pathway begins to exceed the rate for the R → P conformational change. On the basis of this analysis, it has been possible to evaluate the $Cu^{II}L/Cu^{I}L$ self-exchange rate constants associated with both pathways in the proposed square scheme mechanism.

We suggest that most, if not all, Cu(II)/(I) systems involve similar square scheme behavior. Control of the conformational rigidity of specific complexes should make it possible to manipulate the conditions under which gated electron-transfer behavior is observed. Altering the preferred geometry of the coordinating ligand should also make it possible to reverse the preferred pathway for electron transfer so that gating will occur for reduction reactions rather than for oxidations. Studies investigating these possibilities are currently underway.

Acknowledgment. The authors express their appreciation to Dr. Ana M. Q. Vande Linde for initiating the self-exchange rate constant measurements on the $Cu^{II/I}([14]aneS_4)$ complex. The technical assistance of Dr. Mohamad B. Ksebati and the support of the Central Instrument Facility at Wayne State University are gratefully acknowledged. The nuclear magnetic resonance spectrometer utilized for the kinetic measurements was purchased through an equipment grant from the National Science Foundation. Modifications to the stopped-flow spectrophotometer were funded by an unrestricted grant from ICI Americas.

Supplementary Material Available: Original stopped-flow kinetic data and nuclear magnetic resonance line-broadening data (7 pages). Ordering information is given on any current masthead page.